Cerebral amyloid-β PET with florbetaben (^{18}F) in patients with Alzheimer's disease and healthy controls: a multicentre phase 2 diagnostic study

*Henryk Barthel, Hermann-Josef Gertz, Stefan Dresel, Oliver Peters, Peter Bartenstein, Katharina Buerger, Florian Hiemeyer, Sabine M Wittemer-Rump, John Seibyl, Cornelia Reininger, Osama Sabri, for the Florbetaben Study Group**

Lancet Neurol 2011; 10: 424–35

Published Online
April 11, 2011
DOI:10.1016/S1474-4422(11)70077-1

See Comment page 397

*Investigators listed at end of paper

Department of Nuclear Medicine (H Barthel MD, O Sabri MD) **and Department of Psychiatry** (H-J Gertz MD), **University of Leipzig, Leipzig, Germany; Department of Nuclear Medicine, Helios Hospital Berlin-Buch, Berlin, Germany** (S Dresel MD); **Department of Psychiatry and Psychotherapy, Charité, Campus Benjamin Franklin, Berlin, Germany** (O Peters MD); **Department of Nuclear Medicine** (P Bartenstein MD) **and Institute for Stroke and Dementia Research** (K Buerger MD), **Ludwig-Maximilian University, Munich, Germany; Bayer Schering Pharma AG, Berlin, Germany** (F Hiemeyer PhD, S M Wittemer-Rump PhD, C Reininger MD); **and Molecular NeuroImaging, New Haven, CT, USA** (J Seibyl MD)

Correspondence to:
Dr Henryk Barthel, Department of Nuclear Medicine, University of Leipzig, Liebigstrasse 18, 04103 Leipzig, Germany
henryk.barthel@medizin.uni-leipzig.de

Summary

Background Imaging with amyloid-β PET can potentially aid the early and accurate diagnosis of Alzheimer's disease. Florbetaben (^{18}F) is a promising ^{18}F-labelled amyloid-β-targeted PET tracer in clinical development. We aimed to assess the sensitivity and specificity of florbetaben (^{18}F) PET in discriminating between patients with probable Alzheimer's disease and elderly healthy controls.

Methods We did a multicentre, open-label, non-randomised phase 2 study in 18 centres in Australia, Germany, Switzerland, and the USA. Imaging with florbetaben (^{18}F) PET was done on patients with probable Alzheimer's disease (age 55 years or older, mini-mental state examination [MMSE] score=18–26, clinical dementia rating [CDR]=0·5–2·0) and age-matched healthy controls (MMSE ≥28, CDR=0). Our primary objective was to establish the diagnostic efficacy of the scans in differentiating between patients with probable disease and age-matched healthy controls on the basis of neocortical tracer uptake pattern 90–110 min post-injection. PET images were assessed visually by three readers masked to the clinical diagnosis and all other clinical findings, and quantitatively by use of pre-established brain volumes of interest to obtain standard uptake value ratios (SUVRs), taking the cerebellar cortex as the reference region. This study is registered with ClinicalTrials.gov, number NCT00750282.

Findings 81 participants with probable Alzheimer's disease and 69 healthy controls were assessed. Independent visual assessment of the PET scans showed a sensitivity of 80% (95% CI 71–89) and a specificity of 91% (84–98) for discriminating participants with Alzheimer's disease from healthy controls. The SUVRs in all neocortical grey-matter regions in participants with Alzheimer's disease were significantly higher ($p<0·0001$) compared with the healthy controls, with the posterior cingulate being the best discriminator. Linear discriminant analysis of regional SUVRs yielded a sensitivity of 85% and a specificity of 91%. Regional SUVRs also correlated well with scores of cognitive impairment such as the MMSE and the word-list memory and word-list recall scores (r –0·27 to –0·33, $p\leq0·021$). *APOE* ε4 was more common in participants with positive PET images compared with those with negative scans (65% *vs* 22% [$p=0·027$] in patients with Alzheimer's disease; 50% *vs* 16% [$p=0·074$] in healthy controls). No safety concerns were noted.

Interpretation We provide verification of the efficacy, safety, and biological relevance of florbetaben (^{18}F) amyloid-β PET and suggest its potential as a visual adjunct in the diagnostic algorithm of dementia.

Funding Bayer Schering Pharma AG.

Introduction

The definite diagnosis of Alzheimer's disease relies on post-mortem histopathological detection of amyloid-β plaques and neurofibrillary tangles.[1] Furthermore, it is postulated that a gradual change in brain amyloid-β steady-state concentrations is the initial event in the disease that launches the amyloid-β cascade, ultimately leading to neurodegeneration and dementia.[2] Thus, an imaging technique capable of detecting amyloid β during life could help lend objectivity to cognitive testing in the diagnosis of Alzheimer's disease[3] and facilitate or enable an accurate diagnosis at a very early or even presymptomatic stage.[4]

Many ongoing phase 2–3 therapeutic trials in Alzheimer's disease are focusing on strategies that reduce brain amyloid-β burden. They provide hope that effective, disease-modifying treatments based on the molecular pathophysiology of Alzheimer's disease might slow its progression. Such strategies, if effective, would need early and accurate diagnosis and clinical algorithms that are more robust than those used at present. Even before the advent of effective treatments, techniques that can accurately diagnose the disease early in its course are desirable, because they would enable study populations to be enriched with patients with confirmed disease and allow treatment trials at earlier disease stages.[5]

Clinical testing is not sufficiently accurate to serve the above purposes. Meta-analyses have shown that only 70–90% of participants fulfilling the National Institute of Neurological and Communicative Diseases and Stroke–Alzheimer's Disease and Related Disorders Association (NINCDS–ADRDA) criteria of probable Alzheimer's

disease have their diagnosis confirmed subsequently by the gold standard of brain histopathology.[6,7] Consequently, it was suggested that clinical testing for Alzheimer's disease should be supplemented by use of biomarkers, such as brain glucose consumption, mesial temporal lobe atrophy, concentrations of amyloid β, tau, or phospho-tau in CSF, or brain amyloid-β load.[3] In this context, within the past few years, brain PET imaging of amyloid β in particular has emerged as a potential technique to provide so-called in-vivo Alzheimer's disease histopathology—ie, to shift the timepoint of accurate diagnosis from post mortem to ante mortem.[8] Several PET tracers that target amyloid β are therefore under intensive clinical testing.

The most widely used PET tracer for imaging amyloid β is ^{11}C-6-OH-BTA-1 (also known as ^{11}C-Pittsburgh compound B or ^{11}C-PiB), developed by Klunk and colleagues.[9] ^{11}C-PiB brain PET imaging trials in human beings have shown that tracer uptake in neocortical brain regions of patients with Alzheimer's disease is substantially greater than that of individuals without dementia,[9] is predictive for conversion to Alzheimer's disease in people with mild cognitive impairment,[10] and correlates with amyloid-β deposition as established post mortem.[9,11,12] The short radioactive half-life of ^{11}C (20 min), however, restricts the use of ^{11}C-PiB to centres with an on-site cyclotron and an appropriate radiochemistry laboratory.

Widespread distribution necessary for routine clinical use requires a radiotracer with a longer half-life. ^{18}F-labelled amyloid-β-targeting tracers with a half-life of 110 min are under development (including florbetaben [^{18}F], an ^{18}F-labelled polyethylene glycol stilbene derivative). Florbetaben (^{18}F) has a high binding affinity to human post-mortem Alzheimer's disease brain homogenates (K_D=6·7 nM), and the first data from studies in human beings have provided convincing diagnostic efficacy in differentiating between people with Alzheimer's disease and healthy controls.[13] The specificity of florbetaben (^{18}F) tracer binding to amyloid β and not to α-synuclein or tau pathology has been established in post-mortem human brain slices by Fodero-Tavoletti and colleagues (personal communication).

Our primary goal was to establish the sensitivity and specificity of independent visual assessment of florbetaben (^{18}F) PET images acquired 90–110 min post injection in differentiating between people with probable Alzheimer's disease and age-matched healthy controls. Our additional objectives were the assessment of other imaging periods (45–60 min and 110–130 min post injection), optimisation of the visual PET image assessment procedure and subsequent scoring system, investigation of quantitative PET data, and assessment of radiotracer safety and tolerability. The apolipoprotein ε4 (*APOE* ε4) allele is a strong risk factor for the development of Alzheimer's disease[14] because it is linked to the formation and clearance of amyloid β. Thus, we also assessed the association between *APOE* ε4 genotype and florbetaben (^{18}F) PET scan results. Furthermore, we studied the relation between cognitive indices of dementia severity and the florbetaben (^{18}F) PET results.

Methods

Participants

Between Aug 1, 2008, and March 31, 2009, we did a multicentre, open-label, non-randomised clinical phase 2 study in 18 centres in Australia, Germany, Switzerland, and the USA. Our study population consisted of men and women of any ethnic group with the features of probable Alzheimer's disease and cognitively non-impaired healthy controls. The clinical diagnosis based on the NINCDS–ADRDA criteria and on the revised Diagnostic and Statistical Manual of Mental Disorders IV criteria served as the standard with which we compared our findings. All participants were 55 years or older and had completed at least 6 years of education. No participant had physical or imaging findings characteristic of another neurological or psychiatric illness or a history of such illness, present or recent drug or alcohol use or dependence, or any other relevant disease or unstable medical disorder. The webappendix (p 2) lists all inclusion and exclusion criteria for this study. All participants in both cohorts underwent a comprehensive clinical and neuropsychiatric examination, including the clinical dementia rating (CDR), the Consortium to Establish a Registry for Alzheimer's Disease (CERAD) test battery (which included the mini-mental state examination; MMSE), and other cognitive tests. During the trial preparation period, neuropsychiatric training was provided to all referring physicians and their staff. All participants provided written, informed consent. Our study was done in accordance with the Declaration of Helsinki after approval of the local ethics committees and radiation protection authorities of all participating centres.

See Online for webappendix

Procedures

Blood samples for *APOE* genotyping were drawn on a voluntary basis. All coding exons of the *APOE* gene were amplified by PCR and the PCR products were sequenced by Sanger dye-terminator sequencing. To ensure high data quality, the sequence was determined from both strands of the PCR product. All sequences were scanned with PolyPhred software (version 6.18) for polymorphic sites and the results were visually inspected with Consed software (version 19.0).

Brain MRIs were acquired for each participant to exclude cerebral lesions or major cerebrovascular disease, both of which constituted exclusion criteria, and to allow anatomical sampling within prespecified volumes of interest for quantification of florbetaben (^{18}F) brain uptake. For that purpose, during the screening period, non-contrast enhanced, three-dimensional volumetric T1-weighted and T2-weighted brain MRIs were obtained in each case with 1·5 or 3·0 Tesla scanners. Magnetic

resonance image quality was continuously controlled through the entire trial by the imaging core laboratory to ensure the adequacy of the T1-weighted MRIs for successful analysis of the PET data. This entailed confirmation of the parameters of the acquisition sequences and visual interrogation of images for the presence of artefacts and adequacy of grey and white matter contrast.

Florbetaben (^{18}F) was manufactured and handled according to good manufacturing practice at qualified PET manufacturing sites with an automated process that included radiolabelling of the non-radioactive precursor (BOC-Stilbenmesylate) with ^{18}F (radioactive fluoride was provided by an on-site cyclotron) and then acid hydrolysis and semipreparative high performance liquid chromatography for purification (radiochemical purity >93%). The radiotracer (specific activity ≥22 GBq/mmol) was delivered to the PET imaging centres in accordance with the applicable regulatory guidelines.

The eligible participants were—within 4 weeks from screening, including establishment of clinical diagnosis—administered a single dose of 300 MBq (equivalent to a mass dose ≤5 mg) ± 20% florbetaben (^{18}F) in a maximum volume of 10 ml as a slow intravenous bolus injection and then a 10 ml saline flush. Brain PET images were acquired in three-dimensional mode with either a stand-alone PET or a PET/CT scanner from 45 to 60 min and from 90 to 130 min post injection. To minimise motion artefacts, the participants' heads were immobilised with the institution's head holder and fixation equipment. The PET data obtained were corrected for radioactive decay, dead time, measured attenuation, and scatter. The resulting image data were reconstructed by means of iterative algorithms. As a prerequisite for our study, all PET imaging sites were visited by the imaging core laboratory to set up the PET scanners. This site set-up visit included review of the rationale, logistics, and documentation of the imaging protocol with both the clinical recruiting and imaging teams on site, establishment of the PET acquisition and reconstruction protocols on the study PET camera, scanning the Hoffman 3D Brain Phantom with this protocol, and optimising processing to achieve a standard level of smoothing for the subsequent pooling of PET data across different sites and different cameras. These data were submitted to the imaging core laboratory to check the integrity of the electronic transfer. During the trial, PET image quality was continuously and intensively monitored for compliance with the PET acquisition and reconstruction protocols, completeness of source documentation, quality of the image, and final suitability for subsequent visual and quantitative analysis.

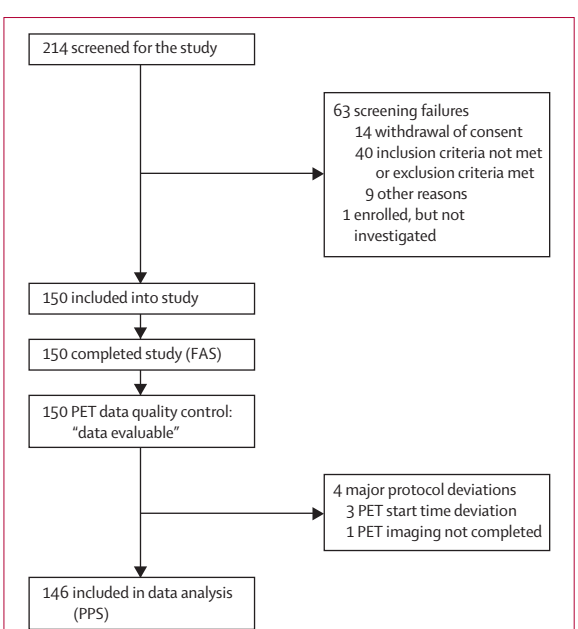

Figure 1: **Study flowchart**
The one participant enrolled but not investigated with florbetaben (^{18}F) PET dropped out because of a mild transitory adverse event before tracer administration. FAS=full analysis set. PPS=per protocol set.

The florbetaben (^{18}F) PET data were visually assessed during a centralised masked read at the imaging core laboratory by three independent brain PET experts who were masked to the clinical diagnosis and all other clinical findings. The summed, 5 min frames 45–60, 90–110, and 110–130 min post injection PET images were assessed in random order interspersed with all other participants' PET imaging periods. Each image was treated as an independent datapoint with a computer-generated randomisation code. The masked read also included a randomised re-read of 10% of the PET image data to check for intrareader reliability—the computer randomisation code treated each time bucket as a separate randomisation pool to select from each of the three time windows equally and these were then added to the overall randomisation pool. Each reader worked at an individual workstation with the RemotEye image viewing system (NeoLogica, Cairo Montenotte, Italy). This system is java-based and accessed via a standard browser on a secure server without internet connection. Readers were permitted to use a greyscale and rainbow colour scale only to review the axial images with operationalised assessment methods. Reader competency was confirmed by individual review of a series of ten test images after training with PET florbetaben (^{18}F) images from a different study. The experts assessed the florbetaben (^{18}F) PET images according to a predefined regional cortical tracer binding (RCTB) scoring system (1=no binding, 2=minor binding, 3=pronounced binding) for eight brain regions (frontal cortex, posterior cingulate, lateral temporal cortex, parietal cortex, occipital cortex, caudate nucleus, mesial temporal cortex, anterior cingulate). The RCTB scores for the frontal cortex, posterior cingulate, lateral temporal cortex, and parietal cortex were then condensed

into a single predefined three-grade scoring system for each PET scan, the brain amyloid-β plaque load (BAPL) score (1=no amyloid-β load, 2=minor amyloid-β load, 3=significant amyloid-β load). The webappendix (p 8) provides further details on the BAPL scoring system. Both the average and the majority read approaches were used for the calculation of diagnostic efficacy, in which a positive PET scan in a patient with Alzheimer's disease was thought to be a match for sensitivity and in a healthy control a negative PET scan a match for specificity. For calculation of the florbetaben (^{18}F) sensitivity and specificity, the so-called average read approach was initially applied and florbetaben (^{18}F) scan results were dichotomised: BAPL scores of 1 and 2 were classified as PET-negative, and BAPL scores of 3 as PET-positive. In further analysis of the data we identified that discrimination between probable Alzheimer's disease and healthy controls could be optimised if the BAPL score was dichotomised such that a score of 1 was classified as PET-negative, and BAPL scores of 2 and 3 were classified as PET-positive. Furthermore, during the course of the trial, we also used the so-called majority read approach to establish the sensitivity and specificity and we report the results obtained from this approach. The webappendix (p 10) lists results with the average read approach. The majority read approach and the latter dichotomisation threshold will also be applied in the phase 2B study and all other ongoing florbetaben clinical trials. The independent masked readers did the visual assessment on the basis of the PET scans alone—ie, without co-registration of MRI brain scans.

	Alzheimer's disease	Healthy controls	p*
Number	81	69	..
Age (years)	70·7 (7·8)	68·2 (6·9)	..
Women	34 (42%)	39 (57%)	..
Education (years)	12·4 (3·1)	14·7 (3·9)	..
Scores on cognitive tests			
MMSE	22·6 (2·3)	29·3 (0·8)	<0·0001
Word-list memory	10·8 (4·7)	22·4 (3·6)	<0·0001
Word-list recall	2·2 (1·9)	8·0 (1·7)	<0·0001
CDR			<0·0001
0·0	0	69 (100%)	..
0·5	29 (36%)	0	..
1·0	49 (60%)	0	..
2·0	3 (4%)	0	..
APOE genotype			<0·0001
ε2/ε2	1 (2%)	1 (2%)	..
ε2/ε3	4 (7%)	13 (20%)	..
ε2/ε4	0	0	..
ε3/ε3	17 (32%)	39 (60%)	..
ε3/ε4	24 (44%)	11 (17%)	..
ε4/ε4	8 (15%)	1 (2%)	..

Data are n (%) or mean (SD). Data are from the full analysis set (n=150), except *APOE* genotype data, which are from 119 participants of the full analysis set who consented to additional genotyping. MMSE=mini-mental state examination. CDR=clinical dementia rating. *APOE*=apolipoprotein E. *Group differences were tested for significance with the two-sided Fisher test for ordinal and the Wilcoxon test for continuous variables.

Table 1: **Study population demographics**

Quantitative PET image analysis was done centrally at the imaging core laboratory by experts who were masked to the participants' clinical diagnoses. An automated segmentation procedure was applied to the three-dimensional T1-weighted MRI scans to remove pixels of high intensity (such as white matter) or pixels of low intensity (such as CSF). Hence, an individualised MRI-based definition of the grey matter was provided. The segmented MRI scan and each PET image were then co-registered with a standard mutual information algorithm and spatially normalised. A modified automated anatomical labelling template[15] was subsequently applied for standardised, regional brain volume of interest sampling of count densities. All analyses were completed in a customised version of PMOD (PMOD Technologies, Zurich, Switzerland) with the exception of MRI segmentation, which used SPM8 (Wellcome Trust Centre for Neuroimaging, London, UK). In three study participants, it was not possible to achieve sufficient grey-matter versus white-matter segmentation by the method applied. As a consequence, these participants were excluded from the below volume of interest definition. Volumes of interest were individually defined on both hemispheres (where appropriate) for the frontal cortex including (separate definition) gyrus rectus and orbitofrontal cortex, temporal cortex including (separate definition) mesial and lateral temporal cortex, parietal cortex, occipital cortex, anterior and posterior cingulate, caudate nucleus, putamen, thalamus, cerebral white matter, pons, cerebellar white matter, and cerebellar cortex. From the regional volumes of interest defined, standardised uptake values were obtained. Dividing the standardised uptake values of the different target regions by that of the cerebellar cortex as reference region resulted in regional standardised uptake value ratios (SUVRs). The cerebellar cortex was chosen as the reference region because of its very low or absent fibrillar amyloid-β deposition on the basis of histopathology and similarity of ^{11}C-PiB PET binding in patients with Alzheimer's disease and healthy controls.[16] Because no hemispherical SUVR asymmetries were detected, we took the mean values of the corresponding left and right hemispherical values. In addition to the regional SUVRs, we established composite SUVRs for each participant, as suggested by Rowe and colleagues,[13] by calculating the mean SUVRs from the frontal, parietal, lateral temporal, anterior and posterior cingulate, and occipital cortices.

Safety assessments included physical examination, vital signs (systolic and diastolic blood pressure, heart rate, and temperature), electrocardiogram, injection-site monitoring, clinical laboratory tests (haematology, serum biochemistry, clotting status, and urinalysis), and

monitoring of adverse events. All assessments were done on the PET imaging day (at prespecified times before and after florbetaben [^{18}F] injection), during the 20–28 h follow-up visit and, as needed, 7 days after administration of florbetaben (^{18}F).

Statistical analysis

Data analysis was done according to a pre-established analysis plan with SAS software (version 9.1). Sensitivity and specificity of the independent visual PET image analysis, including two-sided, normal approximated 95% CIs, were calculated. Pair-wise differences of these variables, together with 95% CIs, between the three different imaging time-windows were assessed with the average masked read approach (webappendix p 14). Inter-reader and intrareader agreements of the visual analysis were estimated by calculating κ coefficients. SUVR group differences between patients with Alzheimer's disease and healthy controls were tested for significance with two-sample *t* tests (including Satterthwaite's approximation of degrees of freedom to account for unequal variances). Effect sizes were expressed as Cohen's *d*. On the basis of the regional SUVR data, a linear discrimination function was selected (webappendix p 9). SUVR differences between visual PET data analysis and *APOE* genotype groups were tested for significances with the Wilcoxon test in the case of continuous data and the two-sided Fisher's exact test in the case of nominal or ordinal data. The relations between regional SUVRs and cognitive scores were expressed as Pearson correlation coefficients for continuous data and Spearman correlation coefficients in the case of ordinal data. Receiver-operating characteristic (ROC) curves were determined with the clinical diagnosis as the standard for comparison and the visual PET data (PET-positive *vs* PET-negative) and *APOE* ε4 genotype (carrying at least one *vs* no *APOE* ε4 alleles) as exploratory variables. The areas under the curves (AUCs) resulting from this ROC analysis were tested for differences according to the approach of DeLong and colleagues.[17] This study is registered with ClinicalTrials.gov, number NCT00750282.

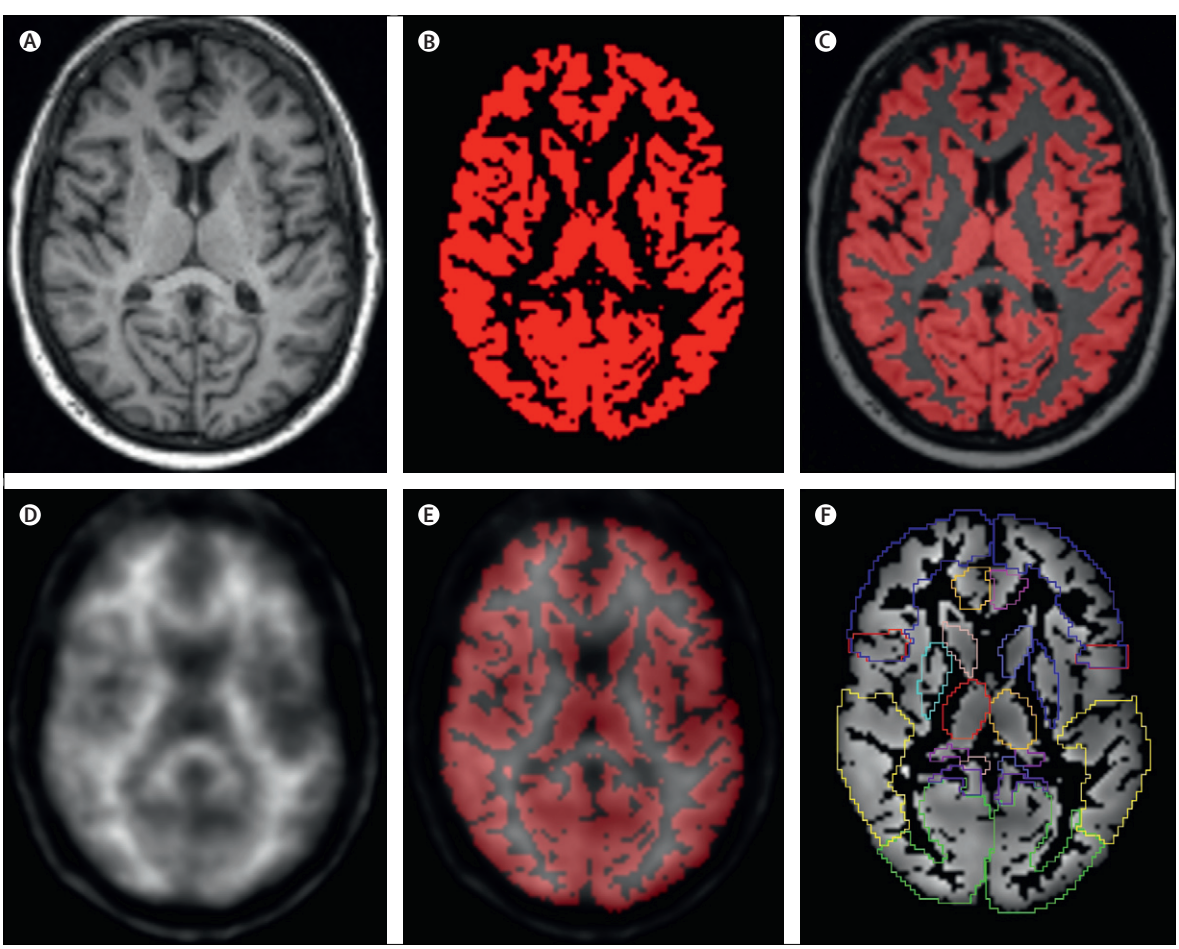

Figure 2: **Quantitative PET data analysis method used**
A typical healthy control's T1-weighted, three-dimensional volumetric MRI (A), the MRI-based grey-matter mask, per se (B) and on respective MRI (C), the participant's florbetaben (^{18}F) PET scan (D), the grey-matter mask transferred to the co-registered florbetaben (^{18}F) PET dataset (E), and the volume of interest set applied to the grey-matter-segmented PET scan (F).

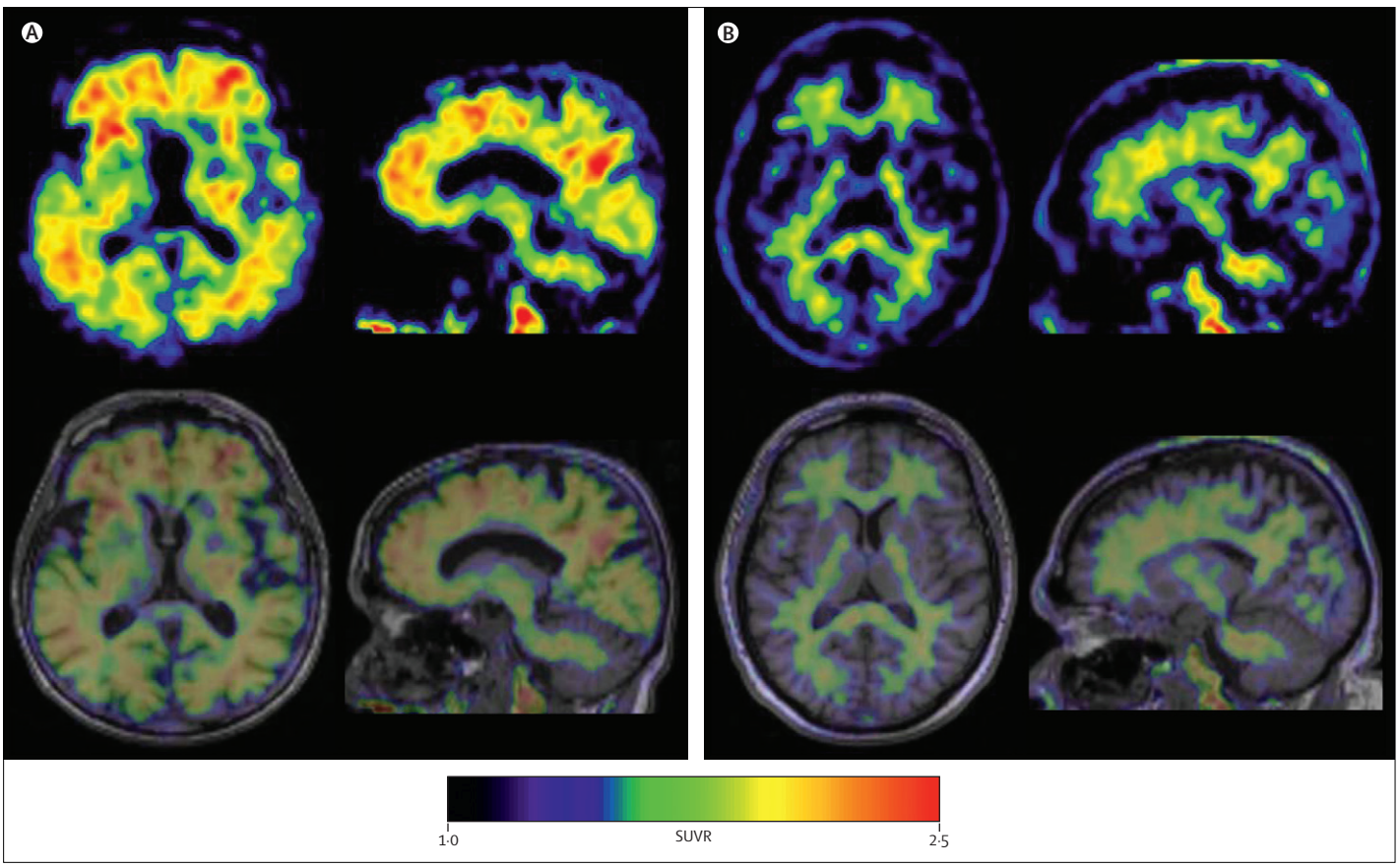

Figure 3: **Paradigmatical florbetaben (^{18}F) PET images**
Axial (left) and sagittal (right) florbetaben (^{18}F) brain PET images (top) and co-registered PET/T1-weighted MRI (bottom), each of a typical Alzheimer's disease patient (A) and a typical healthy control (B). Axial slices are at the level of the basal ganglia; sagittal slices are at the paramedian level. PET images are 90–110 min post injection standardised uptake value ratio (SUVR) data with the cerebellar cortex as reference region. In neocortical brain regions, tracer uptake is apparent in the Alzheimer's disease patient, but not in the healthy control.

Role of the funding source

The study protocol was designed and the study was initiated by the principal investigator (OS) together with the sponsor, who supported the collection, analysis, and interpretation of the data, and who was involved in the writing of the report. The corresponding author and the principal investigator had full access to all the data in the study and had final responsibility for the decision to submit for publication.

	Reader 1	Reader 2	Reader 3
Alzheimer's disease			
BAPL score=1	20 (26%)	17 (22%)	11 (14%)
BAPL score=2	1 (1%)	2 (3%)	8 (10%)
BAPL score=3	57 (73%)	59 (76%)	59 (76%)
Healthy controls			
BAPL score=1	65 (96%)	43 (63%)	56 (82%)
BAPL score=2	1 (2%)	21 (31%)	10 (15%)
BAPL score=3	2 (3%)	4 (6%)	2 (3%)

Data are for the 90–110 min post-injection PET imaging time-window of the per protocol set population. BAPL score 1=no amyloid-β load, 2=minor amyloid-β load, 3=significant amyloid-β load. For the co-primary study endpoint—ie, sensitivity and specificity calculation—the majority results were taken for the three readers. A PET scan was thought to be a match with clinical diagnosis of Alzheimer's disease for BAPL scores of 2 or 3, and a match with a healthy control for a BAPL score of 1. BAPL=brain amyloidβ- plaque load.

Table 2: **Individual results of the three independent masked readers**

Results

Figure 1 shows the study flowchart. Most of the screening failures were participants who were recruited as potential healthy controls but did not meet our cognitive inclusion criteria because of slight cognitive impairment. The webappendix (p 7) lists the screening failures related to not fulfilling inclusion or exclusion criteria. All of the 150 participants included in the study (safety analysis set) received florbetaben (^{18}F), underwent PET scanning, and completed the study (full analysis set; FAS). Table 1 shows the main demographic variables of the FAS population.

Figure 2 shows an illustration of our quantitative PET data analysis method for a typical healthy control and figure 3 shows typical florbetaben (^{18}F) brain PET and co-registered PET/MR images of a patient with

Alzheimer's disease and a healthy control. The characteristic white-matter uptake pattern, without relevant tracer uptake in the cerebral or cerebellar grey-matter regions, was noted in the healthy controls. By contrast with the healthy control, the patient with Alzheimer's disease had tracer accumulation that encompassed the entire neocortex other than the reference region cerebellar cortex.

During the independent masked read, the three reviewers judged all PET images as suitable for assessment. Table 2 lists the single-reader BAPL scores.

According to majority read results, for the 90–110 min post-injection period, 62 of the 78 patients were scored as PET-positive, and 62 of the 68 healthy controls as PET-negative (figure 4). This resulted in a sensitivity of 80% (95% CI 71–89) and a specificity of 91% (84–98; table 3). Apart from a slightly higher sensitivity (3·90%, 95% CI 0·71–7·09) for the 90–110 min post-injection period when compared with the 110–130 min post-injection period, the sensitivity and specificity did not differ significantly across the three PET imaging periods (webappendix p 14). We used a post-hoc statistical modelling approach to account for the imperfection of clinical diagnosis (compared with histopathology), which we used as our standard for comparison. This resulted in an adjusted florbetaben (^{18}F) sensitivity and specificity of 96% and 97%, respectively (90–110 min post-injection period; webappendix p 11). For the nine study centres in which more than five participants were imaged, the sensitivity of the visual PET data analysis ranged from 69% to 100% and specificity from 67% to 100% without signs of major intersite differences (webappendix p 13).

Inter-reader agreement was high, reaching κ values of 0·56 for the 45–60 min post-injection period, 0·60 for the 90–110 min post-injection period, and 0·67 for the 110–130 min post-injection period (each p<0·0001).

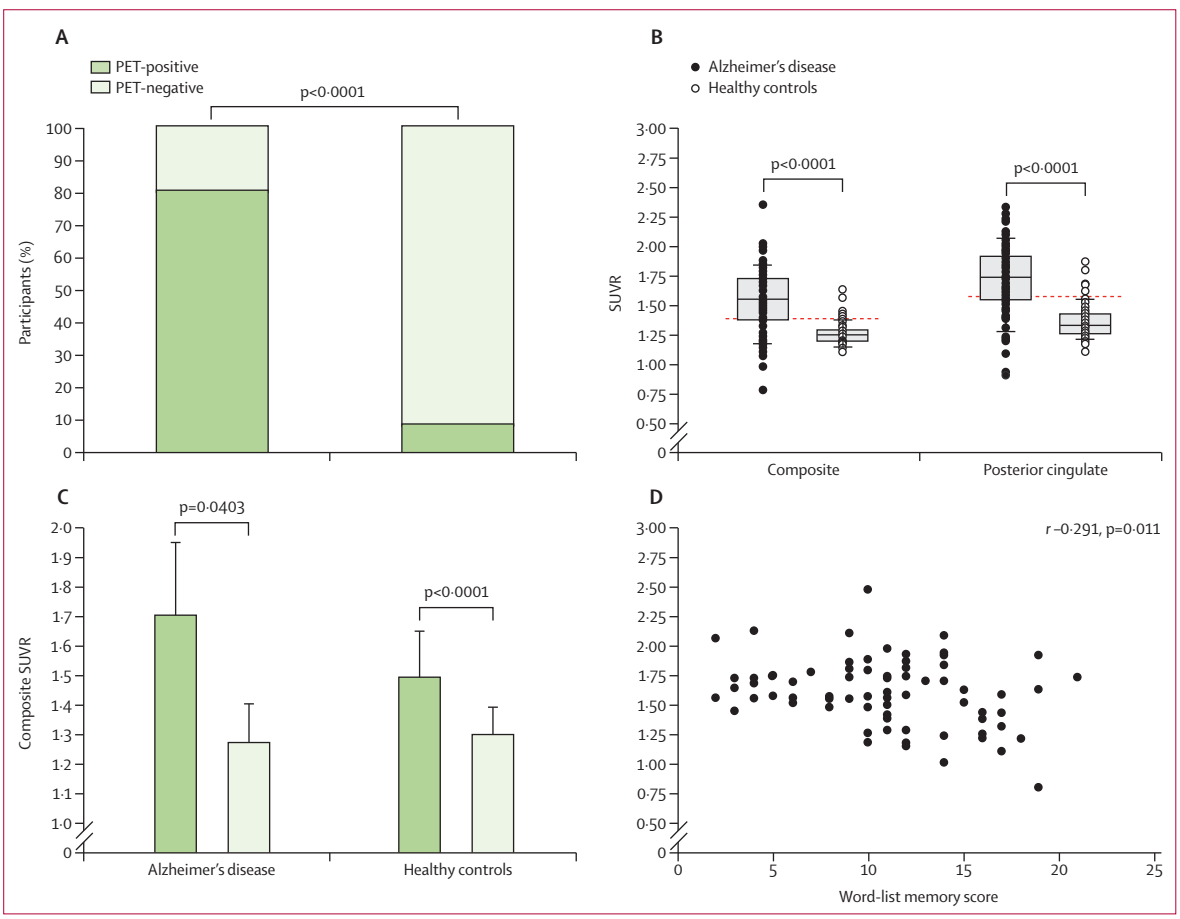

Figure 4: **Visual and quantitative florbetaben (^{18}F) PET image analyses**
(A) Proportion of participants judged PET-positive and PET-negative. (B) Composite and posterior cingulate SUVRs of florbetaben (^{18}F) PET in patients with Alzheimer's disease and healthy controls. Box plots (median, 25% and 75% quartiles) with whiskers with maximum 1·5 IQR, as well as cut-off value (dotted line) for maximum accuracy in group differentiation. For all regional SUVRs, the posterior cingulate SUVRs yielded optimum group discrimination. (C) Comparison of composite SUVRs of florbetaben (^{18}F) PET between PET-positive and PET-negative (according to visual masked read) participants. (D) Association between word-list memory scores of the CERAD battery and composite SUVRs of florbetaben (^{18}F) PET in the Alzheimer's disease patient group. Correlation degree is expressed as Pearson's coefficient. All PET results are 90–110 min post-injection data and were obtained from the per protocol set (n=146). SUVR=standard uptake value ratio. CERAD=Consortium to Establish a Registry for Alzheimer's Disease.

Taking into account the degradation of image quality due to the overall loss of count rates at later acquisition periods, we used the PET results for the 90–110 min post-injection period for the further analyses. The 10% re-read shows high intrareader agreement rates of 98%, 91%, and 91% (overall agreement rate 93%).

For the neocortical brain of patients with Alzheimer's disease, regional SUVRs were significantly higher than those of the healthy controls in frontal, temporal, parietal, occipital, and anterior and posterior cingulate cortices (table 4). Furthermore, the composite SUVRs were also significantly higher for the patients with Alzheimer's disease compared with the healthy controls. Higher SUVRs for the patients with Alzheimer's disease versus healthy controls were also identified in the caudate nucleus and putamen. Lower SUVRs were detected for the patients with Alzheimer's disease compared with the healthy controls in white matter regions, such as cerebral white matter, pons, and cerebellar white matter (table 4). Effect sizes as determined with Cohen's *d* were highest for the posterior cingulate, lateral temporal cortex, composite, parietal cortex, and orbitofrontal cortex. Figure 4 shows the posterior cingulate and the composite SUVRs of patients with Alzheimer's disease and healthy controls. For these quantitative PET variables, the thresholds that optimally separated patients with Alzheimer's disease and healthy controls were 1·57 and 1·39 for the posterior cingulate and composite, respectively. On the basis of the linear discrimination function analysis of the regional SUVRs, a sensitivity of 85% and a specificity of 91% were obtained for the separation between the patients with Alzheimer's disease and healthy controls. For all healthy controls, all neocortical SUVRs were significantly higher (p<0·0001) for the participants visually judged as PET-positive compared with the PET-negative participants. For the patients with Alzheimer's disease, this was also the case for the parietal, occipital, and posterior cingulate cortex SUVRs as well as the composite SUVRs (p=0·0029–0·0403; figure 4; webappendix p 15).

We investigated the relations between the regional and composite SUVRs and three cognition parameters of the CERAD battery (MMSE, word-list memory, and word-list recall scores). We chose the MMSE score for this purpose because it is a widely accepted general indicator of dementia severity.[18] We selected the word-list memory and recall tests because episodic verbal learning and memory, which are assessed by these tests, are usually impaired even in mild Alzheimer's disease.[19] Regional SUVRs were slightly, but significantly, correlated with the MMSE and word-list memory scores, for instance in the lateral temporal cortex (*r* –0·27, p=0·021; *r* –0·33, p=0·004, respectively), and with the word-list recall scores, for instance in the posterior cingulate (*r* –0·27, p=0·019). These correlations were noted only in patients with Alzheimer's disease, and only in neocortical brain regions. Composite SUVRs of the patients with Alzheimer's disease were correlated with the word-list memory (*r* –0·29, p=0·011; figure 4), the word-list recall (*r* –0·24, p=0·040), and the MMSE (*r* –0·23, p=0·048) scores. The webappendix (p 16) lists further results on the relation between florbetaben (¹⁸F) PET data and cognition.

From the 146 participants in the per protocol set, 116 genotypes were available (52 for patients with Alzheimer's disease and 64 for healthy controls). The *APOE* genotype distribution in patients with Alzheimer's

	Alzheimer's disease	Healthy controls	Total	Sensitivity (95% CI)	Specificity (95% CI)
45–60 min post-injection period					
PET-negative	15	61	76	..	..
PET-positive	63	7	70	..	..
Total	78	68	146	81% (72–90)	90% (82–97)
90–110 min post-injection period					
PET-negative	16	62	76	..	..
PET-positive	62	6	70	..	..
Total	78	68	146	80% (71–89)	91% (84–98)
110–130 min post-injection period					
PET-negative	17	61	78	..	..
PET-positive	61	7	68	..	..
Total	78	68	146	78% (69–87)	90% (82–97)

Data are from the per protocol set population. For the classification of the PET scans as normal and abnormal, a brain amyloid-β load score threshold between 1 and 2 was used. 95% CIs for sensitivity and specificity were normal approximated.

Table 3: **Majority read results of the masked read for all three PET imaging periods**

	Alzheimer's disease	Healthy controls	Effect size*	T, p†
Frontal cortex	1·61 (0·32)	1·29 (0·12)	1·28	7·89, <0·0001
Gyrus rectus	1·68 (0·36)	1·33 (0·14)	1·28	7·86, <0·0001
Orbitofrontal cortex	1·66 (0·33)	1·34 (0·12)	1·29	7·93, <0·0001
Temporal cortex	1·52 (0·25)	1·28 (0·10)	1·23	7·54, <0·0001
Lateral temporal cortex	1·57 (0·29)	1·26 (0·11)	1·42	8·73, <0·0001
Mesial temporal cortex	1·41 (0·19)	1·34 (0·10)	0·42	2·58, 0·0112
Parietal cortex	1·53 (0·29)	1·23 (0·12)	1·32	8·10, <0·0001
Occipital cortex	1·49 (0·22)	1·31 (0·09)	1·10	6·74, <0·0001
Anterior cingulate	1·72 (0·35)	1·40 (0·14)	1·19	7·34, <0·0001
Posterior cingulate	1·80 (0·31)	1·42 (0·16)	1·49	9·08, <0·0001
Caudate nucleus	1·40 (0·26)	1·28 (0·14)	0·56	3·41, 0·0009
Putamen	1·69 (0·29)	1·44 (0·13)	1·06	6·52, <0·0001
Thalamus	1·24 (0·24)	1·28 (0·14)	–0·17	–1·04, 0·2996
Cerebral white matter	2·01 (0·30)	2·26 (0·24)	–0·87	–5·56, <0·0001
Pons	1·80 (0·29)	2·02 (0·20)	–0·91	–5·48, <0·0001
Cerebellar white matter	1·88 (0·36)	2·14 (0·22)	–0·87	–5·29, <0·0001
Composite‡	1·62 (0·29)	1·32 (0·11)	1·37	8·43, <0·0001

Values are SUVRs taking the cerebellar cortex as the reference region and expressed as mean (SD). Data are from the 90–110 min post-injection PET imaging period of the per protocol set (n=146). *Cohen's *d*. †T-test using Satterthwaite's approximation of degrees of freedom to account for unequal variances. ‡Arithmetic mean of frontal cortex, lateral temporal cortex, parietal cortex, anterior cingulate and posterior cingulate cortex, and occipital cortex SUVR. SUVR=standardised uptake value ratio.

Table 4: **Quantitative PET data analysis by brain region**

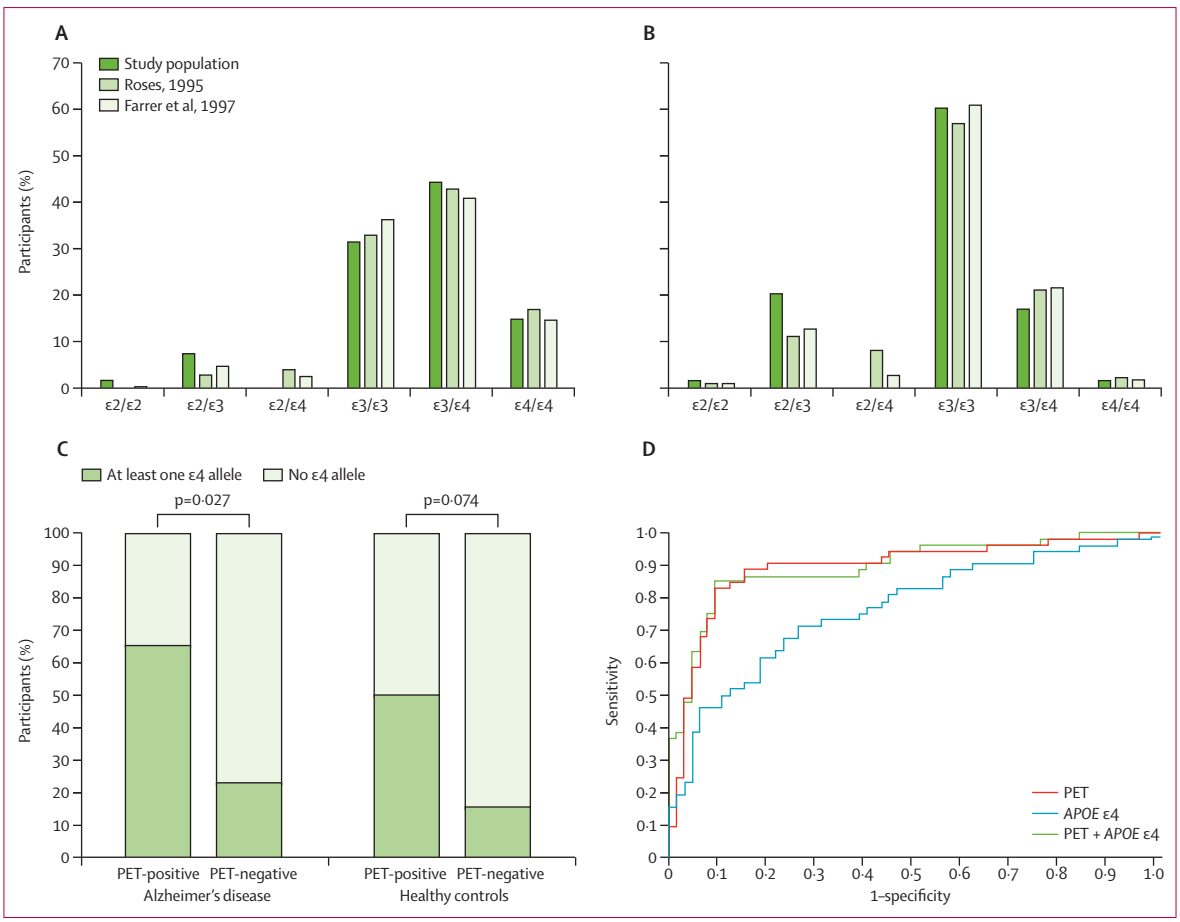

Figure 5: **Association between florbetaben (^{18}F) PET data and apolipoprotein E genotype**
Comparison of *APOE* genotype distribution in patients with Alzheimer's disease (A) and healthy controls (B) between the present study population (n=116) and larger populations as published by Roses[20] (n=276) and Farrer and colleagues[21] (n=11369). Comparison of *APOE* ε4 allele carrier rate between PET-positive and PET-negative participants, separately investigated for patients with Alzheimer's disease and healthy controls. Intergroup significances were tested using the (two-sided) Fisher's exact test (C). Receiver operating characteristic curves for visual florbetaben (^{18}F) PET image analysis, the existence of at least one *APOE* ε4 allele, and a combination of both parameters using the clinical diagnosis as standard for comparison. Areas under the ROC curves were significantly higher for the PET data than for the *APOE* ε4 data (p=0·0063). There was no incremental value of combining both parameters (D). All PET data in this figure were obtained from the 90–110 min post-injection imaging period.

disease and healthy controls was similar to the distribution noted in larger cohorts (figure 5).[20,21] Different patterns were evident for the patients with Alzheimer's disease compared with the healthy controls, with significantly higher frequencies of *APOE* ε4 alleles in favour of the patients with Alzheimer's disease (figure 5).

In patients with Alzheimer's disease with a positive PET result according to the visual masked read, *APOE* ε4 was more common than in patients with Alzheimer's disease with a negative PET result (p=0·027). The same finding was noted in healthy controls, but this did not reach statistical significance (p=0·074). The proportion of participants carrying at least one *APOE* ε4 allele was similar for the PET-positive patients with Alzheimer's disease and PET-positive healthy controls (65% *vs* 50%). The same held for the PET-negative patients with Alzheimer's disease and PET-negative healthy controls (22% *vs* 16%; figure 5) and for the frequency of *APOE* ε2 and ε3 alleles as well as the combinations between the different *APOE* ε alleles in these groups (data not shown).

We did a ROC analysis to investigate how *APOE* ε4 status as an Alzheimer's disease risk factor compares with the florbetaben (^{18}F) PET information with regard to discrimination between Alzheimer's disease and healthy controls, and whether the combination of both variables offers additional value. The florbetaben (^{18}F) PET data yielded a significantly larger AUC than did the *APOE* ε4 genotype (0·89 *vs* 0·76, p=0·0063). Combining the florbetaben (^{18}F) PET data with the *APOE* ε4 status did not further increase the AUC (0·89, p=0·807 compared with the florbetaben [^{18}F] PET AUC; figure 5). In line with these findings, sensitivity and specificity in the 116 participants of the per protocol set from whom the *APOE* genotype could be obtained were 81% and 91%, respectively, for the visual scores of the florbetaben

(^{18}F) PET data and 58% and 81%, respectively, for the *APOE* ε4 genotype.

During the study, 29 treatment-emergent adverse events were reported in ten patients with Alzheimer's disease and 14 healthy controls (16% of the study population). The most common adverse events were injection-site changes related to the route of administration and not to a radiotracer-related sensitivity reaction. Five adverse events (two patients with Alzheimer's disease, three healthy controls) were deemed to be related to the radiotracer: fatigue, feeling hot, increased blood pressure, haematoma, and shaking of both hands. Most adverse events were mild to moderate and resolved during the study period. All laboratory values for serum biochemistry, haematology, and urine analysis data showed general stability over time, with no clinically significant mean changes from baseline or trends indicative of safety concerns. No significant effects of tracer administration on vital signs (heart rate, blood pressure, temperature) and electrocardiogram values were detected (webappendix p 21).

Discussion

Our findings suggest that florbetaben (^{18}F) amyloid-β PET is safe and efficacious in discriminating between patients with Alzheimer's disease and healthy controls. Both visual and quantitative image analysis were shown to deliver practical and sufficiently robust results in a multicamera setting. To the best of our knowledge, this is the first worldwide, multicentre trial and the largest phase 2 trial of an ^{18}F-labelled amyloid-β-targeted PET tracer (panel).

The visual analysis of the multi-PET camera data done by centralised masked read showed good inter-reader and intrareader agreement and indicated high efficacy for florobetan (^{18}F) to discriminate between patients with Alzheimer's disease and healthy controls, with sensitivity and specificity of 80% and 91%, respectively. The sensitivity noted is in the upper range of that which was postulated to be achievable. This is because the clinical diagnosis used in our study as standard for comparison has a restricted positive predictive value (70–90%) when compared with the gold standard post-mortem histopathology.[6,7] We accounted for the imperfection of the clinical diagnosis with an established post-hoc statistical modelling approach. This resulted in adjusted sensitivity and specificity values for florbetaben (^{18}F) PET of 96% and 97%, respectively. Bearing in mind the multicentre design of our trial and the non-invasiveness of this in-vivo imaging technique, these modelling-adjusted values are very promising. They also support the notion that the imperfection of the clinical Alzheimer's disease diagnosis as the standard for comparison needs to be carefully considered in efficacy testing of new diagnostic techniques. However, the further clinical testing of florbetaben (^{18}F) in an ongoing phase 3 trial[24] in which the in-vivo tracer uptake will be compared with post-mortem amyloid-β load will provide pivotal data to further establish the diagnostic potential of this new PET tracer. Furthermore, an additional ongoing trial[25] will reassess the sensitivity and specificity values obtained for florbetaben (^{18}F) in our trial by use of a confirmatory approach. 10% of healthy controls were found to be amyloid-β positive on PET, which is lower than the rate recorded for ^{11}C-PiB (20–30%).[26–29] This is probably because of strict inclusion criteria for both overall cognition and MRI findings (most of our screening failures were healthy controls who did not fulfil these prespecified criteria) and the younger age of the healthy controls.

Diagnostic efficacy did not differ greatly across the three PET imaging periods assessed, suggesting that visual assessment is stable over these periods and that florbetaben (^{18}F) is well suited for routine clinical use, in which a certain flexibility of the imaging period is advantageous. Furthermore, the visual assessment procedure was easily learned by the readers and could be readily incorporated into daily routine on-site PET assessment.

Panel: Research in context

Systematic review

We searched PubMed from 1947 to February, 2011, with the search terms "amyloid PET" and "amyloid imaging", and limited to human studies and clinical trials that tested ^{18}F-labelled tracers that specifically target amyloid β. Proof of concept and dosimetry trials were not considered. Our review revealed only two previously published trials.[22,23] In the first study, which was done as a phase 2 trial in European centres, the PET tracer flutemetamol (^{18}F) was tested in 27 patients with probable Alzheimer's disease, 20 participants with mild cognitive impairment, and 15 healthy controls for its ability to discriminate between patients with Alzheimer's disease and healthy controls. A high discrimination rate was reported. The second study was a phase 3 trial done in North American centres in 29 participants, of whom 15 were pathologically diagnosed with Alzheimer's disease. The brain uptake of florbetapir (^{18}F) as established by PET was correlated with the amount of amyloid β at autopsy. Good correlations were reported.

Interpretation

Our study is the third clinical trial to be reported meeting the above criteria and investigated another ^{18}F-labelled amyloid-β-targeted PET tracer, florbetaben (^{18}F). Our findings verify that florbetaben (^{18}F) can provide accurate differentiation between patients with Alzheimer's disease and healthy controls. Taken together, testing of ^{18}F-labelled amyloid-β-targeted PET tracers both in a large population against the surrogate gold standard of clinical diagnosis and (in a smaller population) against the gold standard of histopathology has provided proof of their efficacy for in-vivo detection of amyloid β in Alzheimer's disease. Future clinical testing will need to establish the prognostic potential of amyloid-β PET tracers in mild cognitive impairment and other prodromal cohorts.

Although visual interpretation of the florbetaben (18F) PET imaging data can deliver accurate diagnostic results, a quantitative PET data analysis might be needed for detection of small amounts of amyloid β in early disease stages as well as for monitoring the effect of amyloid-β-cleaving drugs. In our trial, quantitative PET data generated by means of an MRI-based grey-matter-segmented volume of interest template were able to reproduce the results of the visual PET data analysis. The neocortical tracer uptake was significantly higher for the patients with Alzheimer's disease compared with the healthy controls. On a regional level, best group discrimination was achieved for the posterior cingulate. These results accord with 11C-PiB-PET studies showing posterior cingulate tracer uptake as one of the earliest and most prominent signs of (potentially evolving) Alzheimer's disease.[30,31] These quantitative data successfully replicate in a multicentre phase 2 setting the diagnostic discrimination of patients with Alzheimer's disease and healthy controls reported in a previous single-centre phase 0 study of florbetaben (18F)[13] and in a phase 2 study involving 27 patients with Alzheimer's disease and 15 healthy controls imaged in three centres with another 18F-labelled, amyloid-β targeted tracer.[22] Of importance for future clinical routine use, our study also showed that the accurate quantification of the florbetaben (18F) PET signal is possible in an automated, objective, operator-independent manner.

Correlation of florbetaben (18F) uptake in neocortical brain regions with clinical features such as cognitive impairment might provide useful information on the timing and extent of amyloid-β deposition relevant to Alzheimer's disease clinical phenomenology. We noted slight, but significant correlations, notably only for the patients with Alzheimer's disease, and mainly in the lateral temporal cortex (MMSE, word-list memory) and posterior cingulate (word-list recall), with cognition. The MMSE, word-list memory, and word-list recall scores were chosen as established markers of overall and Alzheimer's disease-specific dementia severity.[18,19] Initial studies in patients with Alzheimer's disease with amyloid-β PET imaging suggested that high levels of amyloid-β accumulation represent an early and effectively unchanging feature of the disease.[32,33] More recent longitudinal studies, however, show a slow increase in amyloid-β deposition in patients with Alzheimer's disease over time.[34] Therefore, the correlations that we have identified might suggest some use of amyloid-β PET as a marker of disease progression, although other brain targets (eg, tau protein or glucose metabolism) might serve this role as well. It needs to be stressed that the correlations noted between the PET data and the cognition scores were only slight, only refer to one secondary study endpoint for which this trial was not powered, and were not corrected for multiple comparisons. More florbetaben (18F) studies in larger populations are therefore needed to further elucidate the PET signal versus cognition association, possibly by including milder cognitive impairment stages and analyses on the individual brain volume affected by amyloid β.

That amyloid-β deposition is a very early feature of the disease and is detectable by PET imaging supports the feasibility of identifying very early Alzheimer's disease or even populations at risk of Alzheimer's disease. Clinical diagnostic algorithms to assess such populations might include high sensitivity screening biomarkers and genetic markers. The *APOE* ε4 represents the main genetic risk factor for the disease that is thought to be directly involved in the formation and clearance of amyloid β.[14] In our study, the *APOE* genotype distribution in both the patients with Alzheimer's disease and healthy controls accords with data published for larger cohorts,[20,21] suggesting a genetically representative study cohort. In the patients with Alzheimer's disease, the partiticpants with positive PET scans had a higher frequency of *APOE* ε4 alleles compared with the PET-negative participants. These findings accord with published data for the PET tracer 11C-PiB.[35,36] For the healthy controls, a similar relation was noted without reaching statistical significance for the study cohort we investigated. The results showing a close association between the florbetaben (18F) PET result and the *APOE* ε4 status support preclinical data for florbetaben (18F) showing that this tracer specifically binds to amyloid β (unpublished data). *APOE* ε4 is clearly an important genetic risk factor for Alzheimer's disease but is not officially recommended for diagnostic purposes. Nevertheless, if one makes the comparison for exploratory purposes, our ROC analysis showed that the florbetaben (18F) PET scan provides better discrimination between patients with Alzheimer's disease and healthy controls than does *APOE* ε4 status. There was no additional improvement when combining both variables, probably due to the high correlation between the florbetaben (18F) PET results and *APOE* ε4 status.

The safety data we gathered suggest that florbetaben (18F) is a safe and well tolerated radiopharmaceutical. These favourable safety data coincide with recently published dosimetry data[37] showing an effective dose well within the range of radiation exposure known for other PET tracers used in clinical practice without major radiation burden concerns.

Contributors

HB, FH, SMWR, JS, CR, and OS contributed to the design of the study. OS was the principal investigator and CR was the study coordinator. HB, HJG, SD, OP, PB, KB, and OS participated in the study as investigators. FH wrote the statistical analysis plan of the protocol and analysed the data. HB, JS, CR, and OS wrote the first draft of the paper. All authors interpreted the data, contributed to the subsequent versions of the article, and approved the final report.

Investigators of the Florbetaben Study Group

Principal investigator—Osama Sabri (University of Leipzig).
Australia—Christopher Rowe, Michael Woodward (Austin Health Melbourne); Barry Chatterton, Robert John Prowse (Royal Adelaide Hospital); George Larcos, Roisin Purcell (Westmead Hospital Sydney).
Germany—Osama Sabri, Henryk Barthel, Hermann-Josef Gertz

(University of Leipzig); Reinhard Ehret (Medical Praxis Neurology Berlin); Alexander Drzezga, Bernd Krause, Alexander Kurz (Technical University Munich); Peter Bartenstein, Dan Rujescu, Katharina Buerger (Ludwig-Maximilian University Munich); Jörg Kotzerke, Michael Bauer (Technical University Dresden); Torsten Kuwert, Johannes Kornhuber (Friedrich-Alexander University Erlangen-Nuremberg); Andreas Bockisch, Hans-Christoph Diener (University of Duisburg-Essen); Jens Wiltfang (LVR Hospital Essen); Stefan Dresel (Helios Hospital Berlin-Buch); Isabella Heuser, Oliver Peters (Charité Berlin); Otmar Schober (University of Münster); Tilman Fey (LWL Hospital Münster); Andreas Bauer (Research Centre Julich); Wolfgang Maier (University of Bonn). *Switzerland*—Alfred Buck, Christoph Hock (University of Zurich). *USA*—Christopher van Dyck, Richard E Carson (Yale University); Danna Jennings, John Seibyl (Institute for Neurodegenerative Disorders New Haven); Susan De Santi, Kent Friedman (New York University); Joshua R Steinerman, Donald Blaufox (Yeshiva University New York).

Conflicts of interest

HB and OS have received consulting fees, honoraria, and travel or accommodation expenses from Bayer Schering Pharma AG. JS discloses equity interest in Molecular Neuroimaging, LLC. OP received payments for lectures from Bayer Schering Pharma AG, Bristol-Myers Squibb, Janssen-Cilag, and Novartis. FH, SMWR, and CR are employees of Bayer Schering Pharma AG. HJG, SD, PB, and KB declare that they have no conflicts of interest.

Acknowledgments

We thank all patients, their caregivers, and the healthy controls who participated in this trial.

References

1 Braak H, Braak E. Neuropathological stageing of Alzheimer-related changes. *Acta Neuropathol* 1991; **82:** 239–59.

2 Haass C, Selkoe DJ. Soluble protein oligomers in neurodegeneration: lessons from the Alzheimer's amyloid β-peptide. *Nat Rev Mol Cell Biol* 2007; **8:** 101–12.

3 Dubois B, Feldman HH, Jacova C, et al. Research criteria for the diagnosis of Alzheimer's disease: revising the NINCDS-ADRDA criteria. *Lancet Neurol* 2007; **6:** 734–46.

4 Dubois B, Feldman HH, Jacova C, et al. Revising the definition of Alzheimer's disease: a new lexicon. *Lancet Neurol* 2010; **9:** 1118–27.

5 Lorenzi M, Donohue M, Paternicò D, et al. Enrichment through biomarkers in clinical trials of Alzheimer's drugs in patients with mild cognitive impairment. *Neurobiol Aging* 2010; **31:** 1443–51.

6 Kukull WA, Larson EB, Reifler BV, et al. The validity of 3 clinical diagnostic criteria for Alzheimer's disease. *Neurology* 1990; **40:** 1364–69.

7 Jellinger K, Danielczyk W, Fischer P, Gabriel E. Clinicopathological analysis of dementia disorders in the elderly. *J Neurol Sci* 1990; **95:** 239–58.

8 Jack CR Jr, Knopman DS, Jagust WJ, et al. Hypothetical model of dynamic biomarkers of the Alzheimer's pathological cascade. *Lancet Neurol* 2010; **9:** 119–28.

9 Klunk WE, Engler H, Nordberg A, et al. Imaging brain amyloid in Alzheimer's disease with Pittsburgh Compound-B. *Ann Neurol* 2004; **55:** 306–19.

10 Wolk DA, Price JC, Saxton JA, et al. Amyloid imaging in mild cognitive impairment subtypes. *Ann Neurol* 2009; **65:** 557–68.

11 Bacskai BJ, Frosch MP, Freeman SH, et al. Molecular imaging with Pittsburgh Compound B confirmed at autopsy: a case report. *Arch Neurol* 2007; **64:** 431–34.

12 Ikonomovic MD, Klunk WE, Abrahamson EE, et al. Post-mortem correlates of in vivo PiB-PET amyloid imaging in a typical case of Alzheimer's disease. *Brain* 2008; **131:** 1630–45.

13 Rowe CC, Ackerman U, Browne W, et al. Imaging of amyloid β in Alzheimer's disease with 18F-BAY94-9172, a novel PET tracer: proof of mechanism. *Lancet Neurol* 2008; **7:** 129–35.

14 Kim J, Basak JM, Holtzman DM. The role of apolipoprotein E in Alzheimer's disease. *Neuron* 2009; **63:** 287–303.

15 Tzourio-Mazoyer N, Papthanassiou D, Crivello F, et al. Automated anatomical labelling of activations in SPM using a macroscopic anatomical parcellation of the MNI single-subject brain. *Neuroimage* 2002; **15:** 273–89.

16 Svedberg MM, Hall H, Hellström-Lindahl E, et al. [11C]PIB-amyloid binding and levels of Aβ40 and Aβ42 in postmortem brain tissue from Alzheimer patients. *Neurochem Int* 2009; **54:** 347–57.

17 DeLong ER, DeLong DM, Clarke-Pearson DL. Comparing the areas under two or more correlated receiver operating characteristic curves: a nonparametric approach. *Biometrics* 1988; **44:** 837–45.

18 Folstein MF, Folstein SE, McHugh PR. "Mini-mental state". A practical method for grading the cognitive state of patients for the clinician. *J Psychiatr Res* 1975; **12:** 189–98.

19 Welsh K, Butters N, Hughes J, Mohs R, Heyman A. Detection of abnormal memory decline in mild cases of Alzheimer's disease using CERAD neuropsychological measures. *Arch Neurol* 1991; **48:** 278–81.

20 Roses AD. Apolipoprotein E genotyping in the differential diagnosis, not prediction, of Alzheimer's disease. *Ann Neurol* 1995; **38:** 6–14.

21 Farrer LA, Cupples LA, Haines JL, et al. Effects of age, sex, and ethnicity on the association between apolipoprotein E genotype and Alzheimer disease. a meta-analysis. *JAMA* 1997; **278:** 1349–56.

22 Vandenberghe R, Van Laere K, Ivanoiu A, et al. 18F-flutemetamol amyloid imaging in Alzheimer disease and mild cognitive impairment: a phase 2 trial. *Ann Neurol* 2010; **68:** 319–29.

23 Clark CM, Schneider JA, Bedell BJ, et al. Use of florbetapir-PET for imaging β-amyloid pathology. *JAMA* 2011; **305:** 275–83.

24 Bayer. Phase III study of florbetaben (BAY94-9172) PET imaging for detection/exclusion of cerebral β-amyloid compared to histopathology—NCT01020838. http://clinicaltrials.gov/ct2/show/NCT01020838 (accessed April 5, 2011).

25 Bayer. Phase II study of florbetaben (BAY 94-9172) PET Imaging for detection/exclusion of cerebral β-amyloid in patients with probable Alzheimer's disease compared to healthy volunteers—NCT00750282. http://clinicaltrials.gov/ct2/show/study/NCT00750282 (accessed April 5, 2011).

26 Pike KE, Savage G, Villemagne VL, et al. β-amyloid imaging and memory in non-demented individuals: evidence for preclinical Alzheimer's disease. *Brain* 2007; **130:** 2837–44.

27 Rowe CC, Ng S, Ackermann U, et al. Imaging β-amyloid burden in aging and dementia. *Neurology* 2007; **68:** 1718–25.

28 Aizenstein HJ, Nebes RD, Saxton JA, et al. Frequent amyloid deposition without significant cognitive impairment among the elderly. *Arch Neurol* 2008; **65:** 1509–17.

29 Jack CR Jr, Lowe VJ, Weigand SD, et al. Serial PIB and MRI in normal, mild cognitive impairment and Alzheimer's disease: implications for sequence of pathological events in Alzheimer's disease. *Brain* 2009; **132:** 1355–65.

30 Mosconi L, Rinne JO, Tsui WH, et al. Increased fibrillar amyloid-β burden in normal individuals with a family history of late-onset Alzheimer's. *Proc Natl Acad Sci USA* 2010; **107:** 5949–54.

31 Ziolko SK, Weissfeld LA, Klunk WE, et al. Evaluation of voxel-based methods for the statistical analysis of PIB PET amyloid imaging studies in Alzheimer's disease. *Neuroimage* 2006; **33:** 94–102.

32 Forsberg A, Almkvist O, Engler H, et al. High PIB retention in Alzheimer's disease is an early event with complex relationship with CSF biomarkers and functional parameters. *Curr Alzheimer Res* 2010; **7:** 56–66.

33 Engler H, Forsberg A, Almkvist O, et al. Two-year follow-up of amyloid deposition in patients with Alzheimer's disease. *Brain* 2006; **129:** 2856–66.

34 Scheinin NM, Aalto S, Koikkalainen J, et al. Follow-up of [11C]PIB uptake and brain volume in patients with Alzheimer disease and controls. *Neurology* 2009; **73:** 1186–92.

35 Drzezga A, Grimmer T, Henriksen G, et al. Effect of APOE genotype on amyloid plaque load and gray matter volume in Alzheimer disease. *Neurology* 2009; **72:** 1487–94.

36 Morris JC, Roe CM, Xiong C, et al. APOE predicts amyloid-beta but not tau Alzheimer pathology in cognitively normal aging. *Ann Neurol* 2010; **67:** 122–31.

37 O'Keefe GJ, Saunder TH, Ng S, et al. Radiation dosimetry of β-amyloid tracers 11C-PiB and 18F-BAY94-9172. *J Nucl Med* 2009; **50:** 309–15.